

## Article (refereed) - postprint

---

Nijse, Femke J.M.M.; Cox, Peter M.; Huntingford, Chris; Williamson, Mark S..  
2019. **Decadal global temperature variability increases strongly with  
climate sensitivity.** *Nature Climate Change*, 9 (8). 598-601.  
<https://doi.org/10.1038/s41558-019-0527-4>

© 2019 Springer Nature Limited

This version available <http://nora.nerc.ac.uk/id/eprint/524582/>

NERC has developed NORA to enable users to access research outputs wholly or partially funded by NERC. Copyright and other rights for material on this site are retained by the rights owners. Users should read the terms and conditions of use of this material at <http://nora.nerc.ac.uk/policies.html#access>

**This document is the author's final manuscript version of the journal article following the peer review process. Some differences between this and the publisher's version may remain. You are advised to consult the publisher's version if you wish to cite from this article.**

<https://link.springer.com/>

Contact CEH NORA team at  
[noraceh@ceh.ac.uk](mailto:noraceh@ceh.ac.uk)

## **Decadal global temperature variability increases strongly with climate sensitivity**

Femke J.M.M. Nijssen, Peter M. Cox, Chris Huntingford and Mark S. Williamson

**Climate-related risks are not only dependent on the warming trend from greenhouse gases, but also on the variability about the trend. However, assessment of the impacts of climate change tend to focus on the ultimate level of global warming<sup>1</sup>, only occasionally on the rate of global warming, and rarely on variability about the trend. Here we show that models which are more sensitive to greenhouse gas emissions i.e. higher equilibrium climate sensitivity (ECS) also have higher temperature variability on time scales of several years to several decades<sup>2</sup>. Counterintuitively, high sensitivity climates, as well as having a higher chance of rapid decadal warming, are also more likely to have had historical ‘hiatus’ periods than lower sensitivity climates. Cooling or “hiatus” decades over the historical period, which have been relatively uncommon, are more than twice as likely in a high ECS world (ECS = 4.5K) compared to a low ECS world (ECS=1.5K). As ECS also affects the background warming rate under future scenarios with unmitigated anthropogenic forcing, the probability of a hyper-warming decade - over ten times the mean rate of global warming for the 20<sup>th</sup> century, is even more sensitive to ECS.**

In this study, we look specifically at the combined effects of climate sensitivity and climate variability, which could stretch the ability of human and natural systems to adapt<sup>3,4,5</sup>. Our approach is to study how decadal trends in global annual mean surface temperature vary with climate sensitivity across the CMIP5 multi-model ensemble<sup>3</sup>. The latter is partially motivated by the 2000-2012 slowdown of surface temperature increase, sometimes known as the ‘warming hiatus’. This slowdown has led some to suggest estimates of ECS below 1.5 K.<sup>4,5</sup> However, rather than making periods of no warming more likely for low climate sensitivities, we show the converse - that

warming slowdowns can be expected more in high sensitivity climates. The background to our claim is the well-known property that a more sensitive dynamical system responds to a perturbation more strongly and is slower to recover than a less sensitive one.<sup>6,7</sup> Forcing from fast random, weather-like perturbations, additional to slow anthropogenic forcing, can push the climate's temperature trend in both warm and cool directions. For more sensitive systems these excursions will be both larger and longer-lived, giving larger and longer-lived temperature trends.

We formalise this intuition by calculating the temperature trend  $b$  ( $\text{K yr}^{-1}$ ) over a window of time  $W$ (yrs), usually a decade. How much the temperature trend varies (quantified as the standard deviation of  $b$ ) with climate sensitivity is the main focus of study in this paper. We follow the approach of using conceptual analytically soluble stochastic climate models to understand the climate system pioneered by Hasselmann and others<sup>8,9</sup>. In particular, we solve for  $b$  and its standard deviation  $\sigma_b$ , using the Hasselmann model which describes the response of the annual global mean surface temperature anomaly  $\Delta T$  (K) to forcing  $Q$  ( $\text{W m}^{-2}$ ):

$$C \frac{d\Delta T}{dt} + \lambda \Delta T = Q$$

where  $Q$  parameterizes fast, internally generated perturbations as a random variable. External driving factors such as anthropogenic forcing due to increases in greenhouse gases may also be included in this term (see methods). The temperature response to  $Q$  depends on the effective heat capacity  $C$  ( $\text{W yr m}^{-2} \text{K}^{-1}$ ) and the climate feedback  $\lambda$  ( $\text{W m}^{-2} \text{K}^{-1}$ ), the latter describing the net effect of all the individual negative and positive feedbacks within the climate. Climates with larger values of  $\lambda$  have a stronger overall negative (restoring) feedback on temperature anomalies and lower equilibrium climate sensitivity  $ECS$  (K).  $ECS$  is defined as the steady-state warming in response to the forcing from a doubling of atmospheric  $\text{CO}_2$  and is inversely proportional to  $\lambda$ :  $ECS = Q_{2\times\text{CO}_2}/\lambda$ . Although the simple Hasselmann model is an imperfect representation of the climate system, it serves here to formulate a hypothesised relationship between variability and  $ECS$ , that we subsequently evaluate against the results from state-of-the-art Earth System Models.

Taking  $Q$  to be given only by stochastic forcing of magnitude  $\sigma_Q$ , analogous to an unforced, control climate model simulation, the Hasselmann model can be solved to first approximation (the full expression is given in the Supplementary Information). This gives a relation for the standard deviation of  $b$  as a function of the trend length  $W$  and climate sensitivity:

$$\sigma_b = \frac{2\sqrt{3}\sigma_Q}{W^{\frac{3}{2}}\lambda} = \text{ECS} \frac{2\sqrt{3}\sigma_Q}{W^{\frac{3}{2}}Q_{2xCO_2}}.$$

As expected, this equation predicts higher variability in warming trends (larger  $\sigma_b$ ) for more sensitive climates (higher ECS). Although the single-box Hasselmann model is a poor representation of warming climates on long time-scales<sup>10</sup>, the two-box model<sup>11</sup>, which better describes oceanic heat storage, produces the same qualitative relationship (Supplementary Methods, Eqn 19). Wigley & Raper (1990)<sup>9</sup> also noted the relation between long term temperature trends and climate sensitivity in numerical simulations of a stochastically forced upwelling diffusion model.

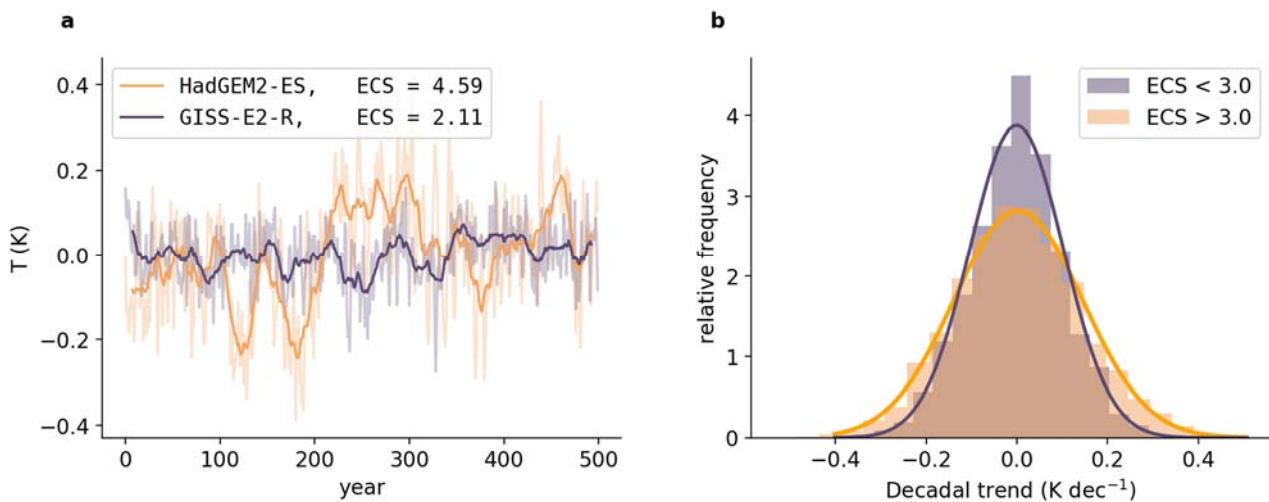


**Figure 1: Decadal variability in global temperature.** *a.* Global mean surface temperature anomaly over a modelled 500-year period with no external forcing, for two control simulations in the CMIP5 database. HadGEM2-ES (brown line) is an example of a model with high climate sensitivity, while GISS-E2-R (purple line) has a low climate sensitivity. Heavy lines are 10 year running means. **b.** Multi-model histograms of decadal variability for low (purple) and high (brown) climate sensitivities in 500 year control simulations. Normal curves fitted to histograms. The individual models are listed in the Table S1 with their climate feedback parameter  $\lambda$  and equilibrium climate sensitivity ECS.

Relating temperature variability to climate sensitivity can be thought of as a heuristic application of the Fluctuation-Dissipation theorem<sup>12,13</sup>, a tool used in many fields of physics.<sup>14</sup> This way of modelling the response to a radiative forcing is complementary to methods that estimate  $\lambda$  as the sum of individual feedbacks. Metrics of variability derived from whole-system approaches can in principle be linked back to individual feedbacks<sup>15,16</sup>.

Observations have been used in combination with simple stochastic climate models to constrain long term variability<sup>9</sup> and ECS<sup>17</sup>. In contrast, we use an ensemble of state of the art climate models (CMIP5 model ensemble<sup>3</sup>) to first look for evidence of this relation in control simulations, before studying its implications in a climate perturbed by fossil fuel burning. Using the control, rather than historical or future simulations, allows for a cleaner test of the hypothesised link between internal variability and sensitivity. This is because historical simulations have additional external forcing and generally simulate shorter periods. Models were included in our analysis if they had a control run spanning at least 500 years. Figure 1a shows the timeseries of annual global mean temperature of a high ECS model (HadGEM2-ES, brown line) and a low ECS model (GISS-E2-R, purple line). The thick line shows the 10 year running mean. The low sensitivity model shows shorter and smaller variation on the decadal timescale, in contrast to the longer and larger temperature trends in the high sensitivity model. Figure 1b shows composite distributions of decadal temperature trends for higher sensitivity (ECS > 3.0 K, brown) and lower sensitivity models (ECS < 3.0K, purple). There is a clear distinction between high and low ECS models, the former having wider histograms indicating more variability in global temperature trends. Previous studies have noted a relationship between tropical decadal temperature variability and sensitivity in the CMIP5 ensemble<sup>18</sup>.

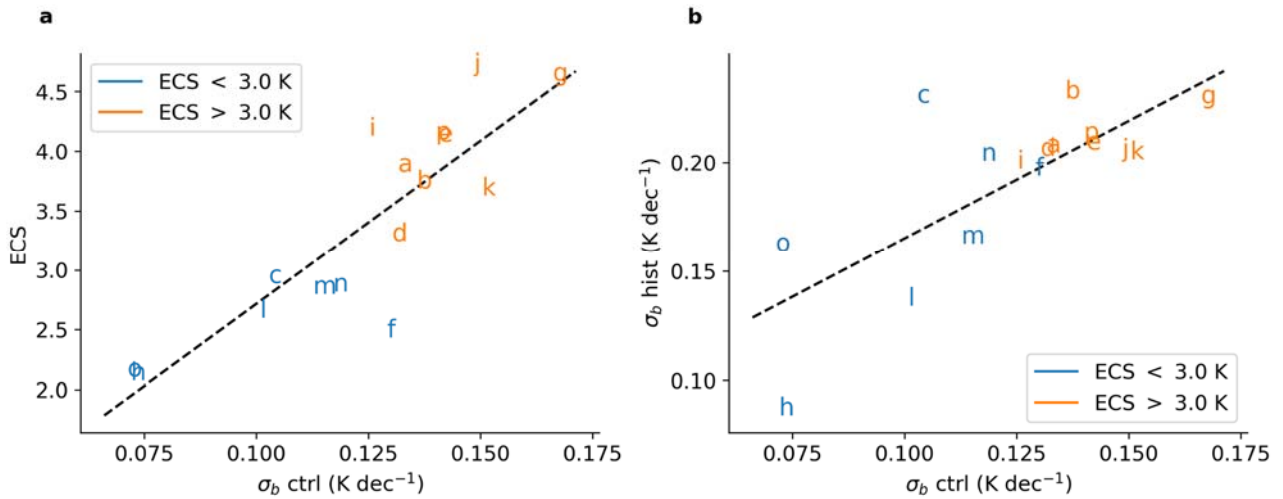


**Figure 2. Emergent relationship between ECS and warming trends. a.** Standard deviation of 10-year temperature trends in an ensemble of 500-yr control runs versus ECS. The dotted line is a linear ordinary least square fit with Pearson  $r=0.86$ . **b.** Ten-year variability in the control runs versus the 10-year variability in the historical period (1881-2017).

In Figure 2a we plot decadal ( $W=10$  years) values of  $\sigma_b$  against ECS for each CMIP5 model control simulation. In Figure 2b standard deviations of decadal trends are plotted for the historical against the control simulations. Decadal trends in the historical simulations are larger due to a non-constant background trend. This causes differing means for the 1880-1950 period compared to the 1950-2012 one. Combining these two periods leads to a larger standard deviation of decadal trends, which explains the larger historical  $\sigma_b$  in Figure 2b. Using all 31 models and model variants in the CMIP5 archive, we find a similar but slightly weaker relationship (see SI Figure 1). While our theory predicts a weakly nonlinear relationship between the standard deviation of trends and ECS, we chose a linear regression between  $\sigma_b$  and ECS to prevent overfitting. Nonlinearities like this may be expected when the dominant time-scale of the climate system and the time-scale of the variability metric are of the same order of magnitude<sup>19</sup>.

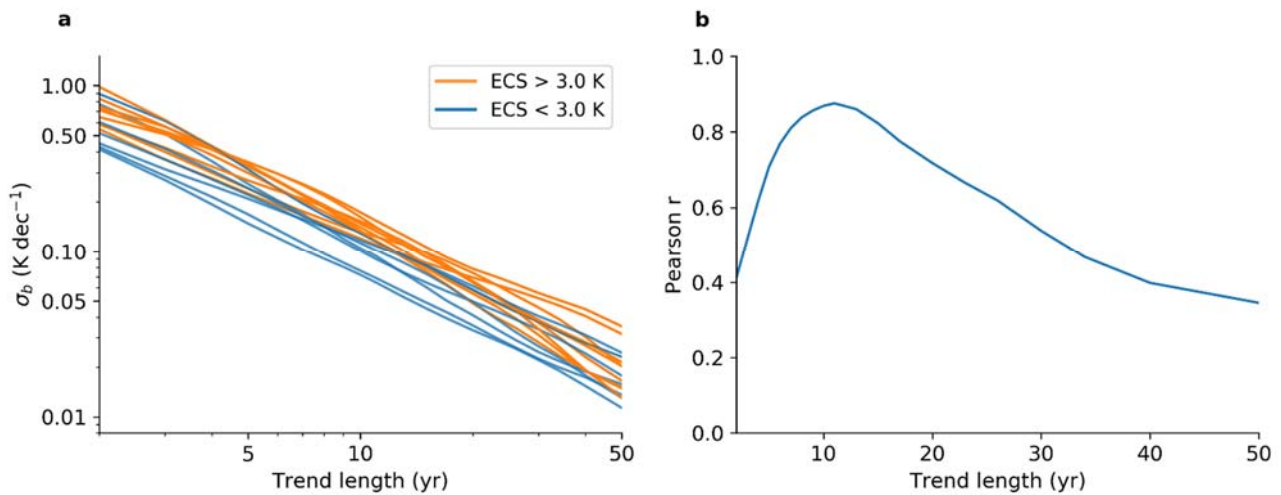


**Figure 3: Varying window lengths.** *a.* log-log plot of trend length versus standard deviation of the trend using the control simulations, differentiated in colour (as marked) between ECS value. *b.* Correlation (Pearson  $r$ ) of the emergent relationship in *a*, between ECS and  $\sigma_b$ , as a function of trend length.

Figure 3a shows the variability of temperature trends of duration 3-50 years. Variability in trends of duration 5-25 years separate the low sensitivity (blue lines, lower variability) and high sensitivity models (orange lines, higher variability). The correlation between ECS and  $\sigma_b$  shown in figure 3b is particularly strong for temperature trends of length 7 to 15 years ( $r > 0.8$ ).

We have explored the possible impact of the El Niño-Southern Oscillation (ENSO) on our ECS versus  $\sigma_b$  correlation, and its dependence on trend length. To characterise ENSO, we use the NINO3.4 index which is based-on temperatures in the region between 120 °W–170 °W and 5 °S–5 °N.<sup>20</sup> By removing the ENSO signal, based on this index, it is shown that ENSO is not the dominant factor in our relationship (Figure S2a). It is notable however that the peak correlation at around 10 years disappears once the ENSO influence is removed, suggesting that the peak is mainly a consequence of ENSO variability. There may also be a smaller contribution to the peak correlation due to longer timescales in the climate response (Figure S3). Excluding ENSO deteriorates the



relationship between  $\sigma_b$  and ECS for all window lengths (Figure S2). This is consistent with ENSO providing a useful additional stochastic forcing of the climate system, which helps to reveal ECS.

Figure 4a plots equal probability contours for anomalies in the decadal temperature change as a function of ECS over the historical period. The probabilities are computed by combining the relationship between the decadal variability and ECS as derived from the control run, with the background warming from the historical runs (Figure S5). Over the historical period (1960-2012) there is a small correlation between the background warming and ECS. Figure 4a is asymmetric, in contrast to Fig S5, because the probability of warming episodes is increased by the ECS-dependent background warming. Figure S4 shows that trends and variability are separable: removing the forced trend by subtracting the mean of initial value ensembles (for those models with a sufficient amount of initial value runs), successfully retrieves the variability found in the control simulations.

Cooling or warming decadal episodes that occur only 5% of the time, show a large sensitivity to ECS. In Figure 4b, corresponding to the grey line in 4a, we plot the probability of a cooling decade assuming a background warming rate consistent with the historical simulations for each model. This includes the weak increase in the warming trend with ECS, as well as the stronger increase in variability with increasing ECS. Even with these two opposing effects, the sensitivity of decadal variability to ECS implies that a ‘hiatus’ period was 2.2 [90% CrI 0.68 – 11] times as likely in a high ECS world (ECS = 4.5K) compared to a low ECS world (ECS=1.5). While some studies indicate that the recent slowdown can partially be explained by a decrease in forcing<sup>21,22</sup>, our results show that even in the case forcing remained constant, a temporarily reduced trend does not imply ECS to be lower.

For a given future scenario of increasing anthropogenic forcing, ECS affects both the mean and the variability in the rate of global warming. Figure 4c plots probability contours for different absolute decadal warming rates as a function of ECS, under the RCP8.5 scenario. Figure 4d shows how ECS

affects the probability of a ‘hyper-warming decade’ – which we define here as one with a warming-rate exceeding  $0.7 \text{ K decade}^{-1}$  (i.e. ten times faster than the mean rate of global warming over the 20<sup>th</sup> century). Whereas a hyperwarming decade very rarely occurs for  $\text{ECS} < 2.5\text{K}$ , it occurs 8% of the time for  $\text{ECS} > 3.5\text{K}$ .

Our findings indicate that the concept of equilibrium climate sensitivity (ECS) is relevant not only to the mean global warming at a given level of atmospheric  $\text{CO}_2$ , but also to temperature variability on decadal timescales. Counter-intuitively, this suggests that the slowdown in global warming from 2002-2012 was more likely in a high ECS world. It also means that decades of very rapid warming, which would stretch the adaptive capacity of ecosystems and society, are also much more likely if ECS is high. A previous constraint based on global temperature variability found a most likely value for ECS at  $2.8 \text{ K}^{23}$ , which is lower than suggested by some other recent studies<sup>16,24,25</sup>. Achieving a better consensus on the risk that we live in a high ECS climate is therefore of critical importance to both the climate mitigation challenge and also to inform efforts to build resilience to climate variability.

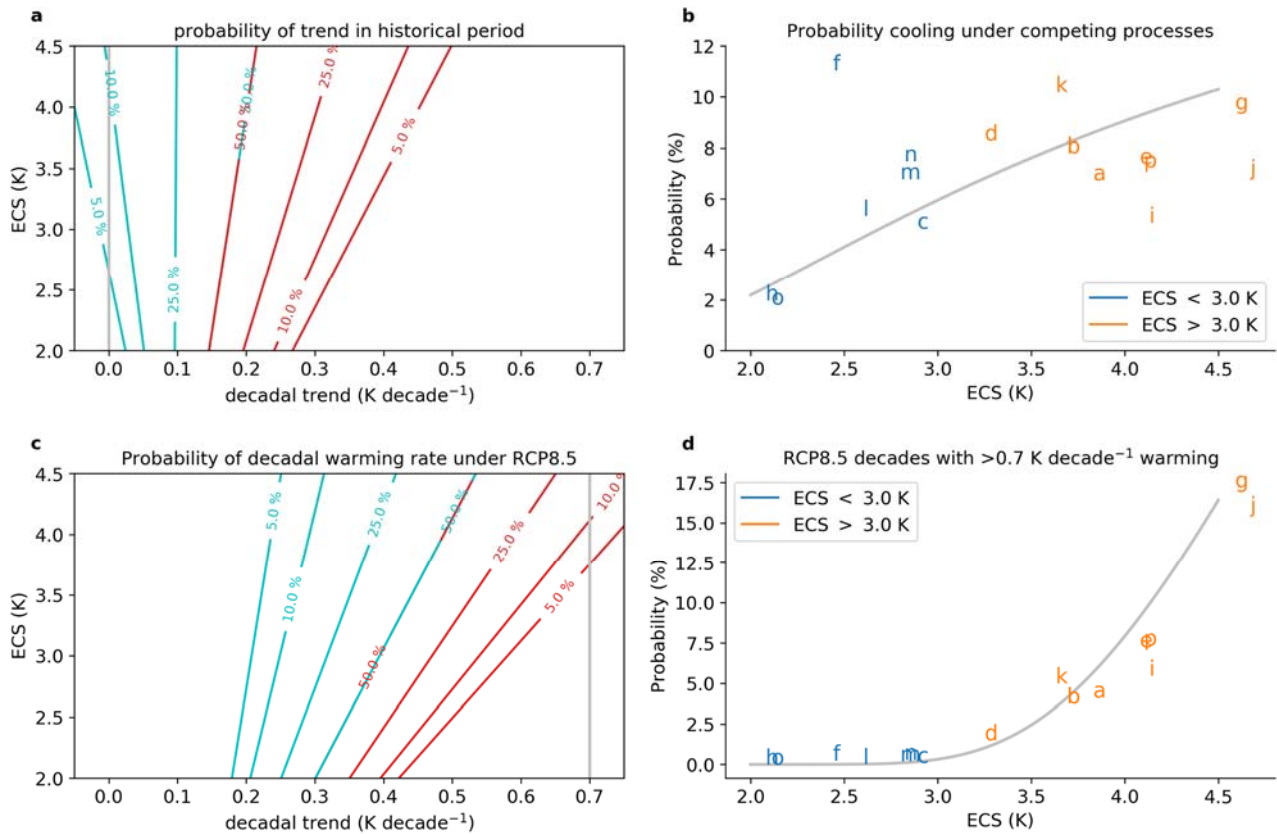


**Figure 4. Probability of warming and cooling.** *a.* Percentage of decades with a larger or equal warming (red) or cooling (blue) rate over the historical period, as computed from the normal distribution using the emergent relationship to estimate standard deviation. *b.* The grey line indicates the probability of having a cooling event over the historical period. The background warming trend for each model was assumed linear in ECS, with the parameters estimated from linear regression between ECS and the modelled 1960-2012 warming rate. The probability of the individual models is computed separately, and marked as letters (key in Table S1) *c.* Dashed blue: chance of a period of cooling in RCP8.5 simulations, colour scheme the same as *a.* *d.* Probability that a decade in RCP8.5 shows hyperwarming:  $0.7 \text{ K decade}^{-1}$  or more (see also vertical gray line in *c*). Colours the same as *b.* The calculations per model are again performed using a normal distribution with a standard deviation estimated from the control runs.

1. United Nations Framework Convention on Climate Change. (1992).

2. Lenton, T. M. Early warning of climate tipping points. *Nat. Clim. Chang.* **1**, 201–209 (2011).
3. Taylor, K. E., Stouffer, R. J. & Meehl, G. A. An overview of CMIP5 and the experiment design. *Bulletin of the American Meteorological Society* (2012). doi:10.1175/BAMS-D-11-00094.1
4. Stocker, T. F., Dahe, Q. & Plattner, G.-K. Technical Summary. in *Climate Change 2013: The Physical Science Basis. Contribution of Working Group I to the Fifth Assessment Report of the Intergovernmental Panel on Climate Change* (2013).
5. Otto, A. *et al.* Energy budget constraints on climate response. *Nat. Geosci.* **6**, 415–416 (2013).
6. Roe, G. Feedbacks, Timescales, and Seeing Red. *Annu. Rev. Earth Planet. Sci.* **37**, 93–115 (2009).
7. Strogatz, S. H. *Nonlinear dynamics and chaos : with applications to physics, biology, chemistry, and engineering.* (Westview Press, 2000).
8. Hasselmann, K. Stochastic Models of Climate Extremes: Theory and Observations. *Tellus* **28**, 473–485 (1976).
9. Wigley, T. M. L. & Raper, S. C. B. Natural variability of the climate system and detection of the greenhouse effect. *Nature* **344**, 324–327 (1990).
10. Caldeira, K. & Myhrvold, N. P. Projections of the pace of warming following an abrupt increase in atmospheric carbon dioxide concentration. *Environ. Res. Lett.* **8**, 34039–10 (2013).
11. Geoffroy, O. *et al.* Transient climate response in a two-layer energy-balance model. Part I: Analytical solution and parameter calibration using CMIP5 AOGCM experiments. *J. Clim.* **26**, 1841–1857 (2013).
12. Leith, C. E. Climate Response and Fluctuation Dissipation. *Journal of the Atmospheric Sciences* **32**, 2022–2026 (1975).
13. Gottwald, G. A., Wormell, J. P. & Wouters, J. On spurious detection of linear response and misuse of the fluctuation–dissipation theorem in finite time series. *Phys. D Nonlinear Phenom.* **331**, 89–101

(2016).

14. Kubo, R. The fluctuation-dissipation theorem. *Reports Prog. Phys.* **29**, 255–284 (1966).
15. Lutsko, N. J. & Takahashi, K. What Can the Internal Variability of CMIP5 Models Tell Us About Their Climate Sensitivity? *J. Clim.* **31**, JCLI-D-17-0736.1 (2018).
16. Caldwell, P. M., Zelinka, M. D. & Klein, S. A. Evaluating Emergent Constraints on Equilibrium Climate Sensitivity. *J. Clim.* JCLI-D-17-0631.1 (2018). doi:10.1175/JCLI-D-17-0631.1
17. Schwartz, S. E. Heat capacity, time constant, and sensitivity of Earth's climate system. *J. Geophys. Res.* **112**, 24–5 (2007).
18. Colman, R. & Power, S. B. What can decadal variability tell us about climate feedbacks and sensitivity? *Climate Dynamics* 1–14 (2018). doi:10.1007/s00382-018-4113-7
19. Nijssen, F. J. M. M. & Dijkstra, H. A. A mathematical approach to understanding emergent constraints. *Earth Syst. Dyn.* **9**, 999–1012 (2018).
20. Roberts, C. D., Palmer, M. D., McNeall, D. & Collins, M. Quantifying the likelihood of a continued hiatus in global warming. *Nat. Clim. Chang.* **5**, 337–342 (2015).
21. Smith, D. M. *et al.* Role of volcanic and anthropogenic aerosols in the recent global surface warming slowdown. **6**, (2016).
22. Medhaug, I., Stolpe, M. B., Fischer, E. M. & Knutti, R. Reconciling controversies about the 'global warming hiatus'. *Nature* **545**, 41–47 (2017).
23. Cox, P. M., Huntingford, C. & Williamson, M. S. Emergent constraint on equilibrium climate sensitivity from global temperature variability. *Nature* **553**, 319–322 (2018).
24. Brown, P. T. & Caldeira, K. Greater future global warming inferred from Earth's recent energy budget. *Nature* **552**, 45–50 (2017).

25. Sherwood, S. C., Bony, S. & Dufresne, J. L. Spread in model climate sensitivity traced to atmospheric convective mixing. *Nature* **505**, 37–42 (2014).

### **Additional information**

Correspondence and requests for materials should be addressed to F.J.M.M.N.

### **Acknowledgements**

This work was supported by the European Research Council (ERC) ECCLES project, grant agreement number 742472 (F.J.M.M.N. and P.M.C.); the EU Horizon 2020 Research Programme CRESCENDO project, grant agreement number 641816 (P.M.C. and M.S.W.); and the NERC CEH National Capability fund (C.H.). We also acknowledge the World Climate Research Programme's Working Group on Coupled Modelling, which is responsible for CMIP, and we thank the climate modelling groups (listed in Table S1 of this paper) for producing and making available their model output.

### **Author contributions**

All authors contributed towards the design of the study and aided in writing the manuscript. F.J.M.M.N. led on the theoretical analysis, C.H. led on the time-series data.

## **Methods:**

### **Data selection**

We selected models based on a set of three criteria.

1. Maximum of one model per modelling group to avoid bias towards certain modelling centres.
2. Top of the atmosphere fluxes and forcing at 4xCO<sub>2</sub> should be available so that it can be tested that ECS is independent of internal forcing strength.
3. There must be at least 500 years of control data available.

For all models with more than 500 years, the last 500 years were chosen. Note that drift, if linear, does not affect the metric  $\sigma_b$ .

### **Calculation of probabilities**

The background warming for the historical period and future projections were computed using OLS linear regression between the temperature change and ECS. The temperature change itself was also computed using OLS linear regression between annual temperatures and time. Temperature time-series in models with multiple initial value members were averaged before a warming rate was computed.

In the second step, the emergent relationship between ECS and  $\sigma_b$  from the control simulations was used. Using a normal distribution for the decadal trend with the standard deviation dependent on ECS, probabilities are computed for either a period of cooling or a period of warming. In the case of an ECS-dependent background rate, the mean of the distribution is adjusted. This procedure is used for figure 4.

Finally, for the comparison of probabilities, i.e. the comparison of probability to have a decade of decreasing temperatures in a high ECS world, versus a low ECS world, a Bayesian linear regression was used for the emergent relationship using the STAN software. Weakly informative priors were used.<sup>26</sup> This allowed us to get a collection of linear fits between  $\sigma_b$  and ECS. Note that in this collection, there are fits with a shallower and steeper slope compared to OLS linear regression. This translates into a having both high  $\sigma_b$  for low ECS and a low  $\sigma_b$  for high ECS in the shallow fits and visa versa for the steeper fits. From these pairs, pairs of probabilities of cooling decades are computed (as described in the previous paragraph), and these are divided to compute how much more likely a period of cooling is in a high ECS world compared to a low ECS world. Using pairs of regression lines leads to a larger estimate of uncertainty than a naïve approach with OLS regression would have.

### **Analysis effect ENSO**

The effect of ENSO was studied by regressing out the NINO3.4 index. A linear regression between GMST and NINO3.4 was first performed, and then decadal trends were computed using the GMST residuals.

### **Analytic relationship ECS and variation trend.**

A trend  $b$  of a  $W$ -yr time series is computed using an ordinary least squares fit of the timeseries. The slope  $b$  in such a fit is given by:

$$b = \frac{\text{Covar}(T_t t)}{\text{Var}(t)}$$

Where  $T_t$  is the temperature at time  $t$ . To obtain an analytical solution for the typical size of a trend  $b$  in the absence of external forcing, the standard deviation  $\sigma_b$ , we write the Hasselmann model as a stochastic differential equation (SDE) where  $Q$  parametrized as a white noise process (the derivative of a Wiener process  $W$ ) with standard deviation  $\sigma_Q$ .



$$CdT = -\lambda T dt + \sigma_Q dW$$

Using the Green's function associated with this Stochastic Differential Equation, namely  $G_{Hasselmann}$   $= 1/C e^{-t/\tau}$ ,  $\tau = C/\lambda$ , we can write down the solution of temperature as a stochastic integral i.e.

$$T_t = \sigma_Q \int_0^t G_{Hasselmann}(t-s) dW_s$$

Using this solution we can now find  $b$  and its standard deviation for a trend of  $W$  years.

Multiple steps of algebraic manipulation, which are given in the Supplementary Information, then lead to

$$Var[b] = \frac{12\sigma_Q^2}{W^3\lambda^2} (1 - f(\tau, W))$$

To first order,  $\sigma_b$  is linearly proportional to  $1/\lambda$ , which is in turn proportional to equilibrium climate sensitivity, defined as  $ECS = Q_{2\times CO_2}/\lambda$ . The smaller  $W$  is, however, the more deviations towards nonlinearity occur.

A similar result can be obtained when a deep ocean layer is added to give a two-box model<sup>11</sup>.

$$CdT = (-\lambda T - \gamma(T - T_0))dt + \sigma_Q dW$$

$$C_0 dT = \gamma(T - T_0)dt$$

Here the zero subscript denotes the deep ocean layer and  $\gamma$  is a heat exchange parameter. The Green's function for the top layer is<sup>27</sup>:

$$G_T = \frac{1}{\lambda} \left( \frac{a_f}{\tau_f} e^{-\frac{t}{\tau_f}} + \frac{a_s}{\tau_s} e^{-\frac{t}{\tau_s}} \right)$$

With  $\tau_f$  and  $\tau_s$  denoting the fast and slow time scales and  $a_f$  and  $a_s$  the partial contribution of the fast and the slow mode to the response. Similarly to the Hasselmann model,  $\sigma_b$  is proportional to  $\frac{1}{\lambda}$  to first order.

$$\text{Var}[b] = \frac{12}{\lambda^2 W^3} \sigma_Q^2 (1 - g(C, C_0, \lambda, \gamma, W))$$

**Data availability.** The datasets generated during the current study are available from the corresponding author on reasonable request.

**Code availability.** The Python code used to produce the figures in this paper is available from the corresponding author on reasonable request.

Additional references:

26. Stan Development Team. Stan Modeling Language Users Guide and Reference Manual, Version 2.18.0. (2018).
27. Williamson, M. S., Cox, P. M. & Nijssen, F. J. M. M. Climate Sensitivity and Global Temperature Variability in Conceptual Models. *Dyn. Stat. Clim. Syst.* 1–13 (2018).  
<https://doi.org/10.1093/climsys/dzy006>